Arabian Journal of Chemistry (2015) **8**, 343–354

King Saud University

Arabian Journal of Chemistry

www.ksu.edu.sa
www.sciencedirect.com

ORIGINAL ARTICLE

Recent developments in preparation of activated carbons by microwave: Study of residual errors

Ashly Leena Prasad [a], **T. Santhi** [a,*], **S. Manonmani** [b]

[a] *Department of Chemistry, Karpagam University, Coimbatore 641 021, India*
[b] *Department of Chemistry, PSG College of Arts and Science, Coimbatore 641 014, India*

Received 8 December 2010; accepted 18 January 2011
Available online 22 January 2011

KEYWORDS

Acacia nilotica;
Adsorption;
Equilibrium isotherm;
Non-linear regression;
Kinetics;
Desorption

Abstract The application of microwave activated *Acacia nilotica* leaves (MVM) and chemically activated *A. nilotica* leaves (CVM) for the removal of crystal violet (CV) from aqueous solution was studied in a batch system. Equilibrium sorption isotherms and kinetics were investigated. The applicability of the Langmuir model for CV onto CVM and MVM was proved by the high correlation coefficient and non-linear regression such as, residual root mean square error (RMSE), chi-square (χ^2), sum of the square of the errors (ERRSQ), composite functional error (HYBRD), derivative of Marquardt's percent standard deviation (MPSD), average relative error (ARE), sum of absolute error (EABS) and average percentage error (APE). The adsorption of CV onto CVM and MVM follows pseudo-second-order kinetic model with intraparticle diffusion is one of the rate-limiting steps. The adsorption capacity of MVM is greater than CVM. The preparation of MVM is agreeing with the principles of green chemistry. Therefore, the eco friendly adsorbent MVM is expected to be the environmentally and the economically feasible adsorbent for the removal of CV from aqueous solution.

1. Introduction

The textile industries are the greatest generators of liquid effluent due to the high quantity of water used in the dyeing process (Selen et al., 2008). Dyes used in textile industries may be toxic to aquatic organisms and can be resistant to natural biological degradation. Hence, the removal of color synthetic organic dyestuff from waste effluents becomes environmentally important (Hameed, 2009). The valorization of agricultural wastes into valuable materials without generating pollutants is a big challenge and recommended for an industrial sustainable development in order to preserve the environment (Reffas et al., 2010).

Adsorption has been shown to be one of the most promising and extensively used methods for the removal of both inorganic and organic pollutants from contaminated water. Adsorption onto activated carbon is proven to be very effective in treating textile wastes. However, in view of the high cost and associated problems of regeneration, there is a constant search for alternate low-cost adsorbents (Madhavakrishnan

* Corresponding author. Tel.: +91 04222401661; fax: +91 04222611146.
E-mail address: ssnilasri@yahoo.co.in (T. Santhi).
Peer review under responsibility of King Saud University.

ELSEVIER Production and hosting by Elsevier

1878-5352 © 2011 Production and hosting by Elsevier B.V. on behalf of King Saud University.
http://dx.doi.org/10.1016/j.arabjc.2011.01.020

et al., 2009). But those adsorbents were chemically activated and sometimes it may cause other environmental hazards.

Acacia nilotica is a species of *Acacia*, native to Africa and the Indian subcontinent. In Haryana, *A. nilotica* based agro forestry systems reduced the yield of wheat (Puri et al., 1995). The aim of the paper is to find out the more suitability and applicability of carbon prepared by different activation (microwave and chemical) of *A. nilotica* to uptake cationic dye (crystal violet) from simulated waste water. The microwave activation method was used because of its one-step simple process and the approach toward green chemistry principle.

Discharge of CV into the hydrosphere can cause environmental degradation, because CV is readily absorbed into fish tissue from water exposure and is reduced metabolically by fish to the leuco moiety, leucocrystal violet (LCV). Several studies by the National Toxicology Program reported that the carcinogenic and mutagenic effects of crystal violet in rodents. It has also been linked to increased risk of human bladder cancer. The leuco form induces renal, hepatic and lung tumor in mice.

There are two main objectives of this study: the first is to prepare an eco friendly microwave activated carbon based on *A. nilotica* leaves as an agricultural waste for the depollution of water effluents contaminated by dyes from textile industry; the second is to compare the adsorption properties of microwave activated carbon with chemically activated carbon based on *A. nilotica* leaves. Desorption was used to elucidate the nature of adsorption and to design the mechanism for recycling of the spent adsorbent.

2. Materials and methods

2.1. Preparation of adsorbent and adsorbate

The leaves of *A. nilotica* were dried in an oven and treated with conc. H_2SO_4 for 12 h and washed thoroughly with distilled water till neutral pH is attained and soaked in 2% $NaHCO_3$ overnight in order to remove any excess of acid present. Then the material (CVM) was washed with distilled water and dried. The raw sample is placed in a microwave oven (Samsung; Triple Distribution System) at 800 W for 2 min. The carbonized sample (MVM) was collected. Both CVM and MVM were preserved in an air tight container for further studies.

The commercial grade crystal violet (color index No. 42555) with molecular formula $C_{25}H_{30}ClN_3$, molecular weight 407.99 and λ_{max} 584 nm are obtained from Thomas baker (chemicals) Ltd., Mumbai, India (Fig. 1). All the chemicals used throughout this study were analytical-grade reagents and the adsorption experiments were carried out at room temperature (27 ± 2 °C).

2.2. Characterization of CVM and MVM

The surface morphology and fundamental physical properties of the sorbents were obtained by the scanning electron microscope (LEO 435 VP model) and Fourier Transform Infrared (FTIR) analysis. Determination of zero point charge (pH_{zpc}) was done to investigate the surface charge of both chemically and microwave activated adsorbents for different solution pH.

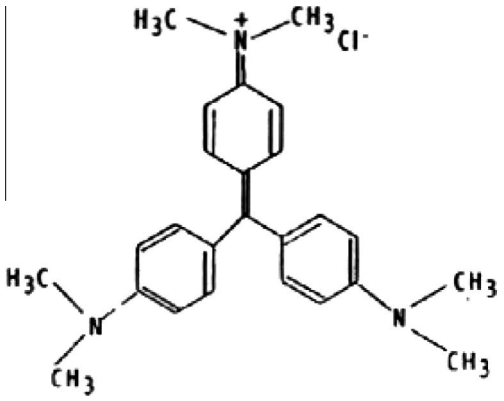

Figure 1 Structure of crystal violet dye.

2.3. Batch adsorption studies

The adsorption experiments were carried out in a batch process to evaluate the effect of pH, contact time, adsorbent dose, adsorption kinetics, adsorption isotherm and desorption of CV onto CVM and MVM.

2.3.1. Dye uptake experiments

For each experiment, a series of flasks were prepared with 50 mL of dye solution (25–200 mg/L, respectively) and the pH was adjusted from 2 to 8 using a pH meter (Deluxe pH meter, model-101 E). About 0.2 g of the sorbent was added, and the flasks were agitated at 160 rpm. The sorbent was removed by centrifugation and the supernatant was analyzed using a Systronic Spectrophotometer-104 at wavelength of 584 nm. Desorption studies were carried out by filtering the dye loaded adsorbent and the percentage of desorption was analyzed.

The amount of dye adsorbed at equilibrium onto carbon, q_e (mg g^{-1}) was calculated by the following mass balance relationship:

$$q_e = (C_0 - C_e)V/W \quad (1)$$

where C_0 and C_e are the concentrations (mg L^{-1}) of CV at initial and equilibrium, respectively. V is the volume (L) of the solution and W is the weight (g) of the adsorbent used.

2.3.2. Determining isotherm parameters by non-linear regression

Due to the inherent bias resulting from linearization, alternative isotherm parameter sets were determined by non-linear regression. This provides a mathematically rigorous method for determining isotherm parameters using the original form of the isotherm equation (Khan et al., 1996; Malek and Farooq, 1996; Seidel and Gelbin, 1988; Seidel-Morgenstern and Guichon, 1993). Non-linear analysis of isotherm data is an interesting mathematical approach for describing adsorption isotherms at constant temperature for water and waste water treatment applications and to predict the overall sorption behavior under different operating conditions (Hadi et al., in press). Indeed, as different forms of the equation affected R^2 values more significantly during the linear analysis, the non-linear analysis might be a method of avoiding such errors (Ncibi, 2008). Most commonly, algorithm based on the Levenberg–Marquardt or Gauss–Newton methods are used (Ho, 2004).

In this study, eight non-linear error functions were examined and in each case a set of isotherm parameters were determined by minimizing the respective error function across the concentration range studied. The error functions employed were as follows:

(i) Residual root mean square error (RMSE)

$$\sqrt{\frac{1}{n-2}\sum_{i=1}^{N}(q_{e(exp)}-q_{e(cal)})^2} \tag{2}$$

(ii) The chi-square test

$$\chi^2=\sum_{i=1}^{N}\frac{(q_{e(exp)}-q_{e(cal)})^2}{q_{e(cal)}} \tag{3}$$

If data from the modal are similar to the experimental data, χ^2 will be a smaller number; if they are different, χ^2 will be a large number. The subscript "exp" and "cal" shows the experimental and calculated values and N is the number of observations in the experimental data. The smaller the RMSE value, the better the curve fitting (Tsai and Juang, 2000).

(iii) The sum of the square of the errors (ERRSQ)

$$\sum_{i=1}^{N}(q_{e(exp)}-q_{e(cal)})_i^2 \tag{4}$$

(iv) A composite fractional error function (HYBRD)

$$\sum_{i=1}^{N}\left[\frac{(q_{e(exp)}-q_{e(cal)})^2}{q_{e(exp)}}\right]_i \tag{5}$$

(v) A derivative of Marquardt's percent standard deviation (MPSD)

$$\sum_{i=1}^{N}\left[\frac{(q_{e(exp)}-q_{e(cal)})}{q_{e(exp)}}\right]_i^2 \tag{6}$$

(vi) The average relative error (ARE)

$$\sum_{i=1}^{N}\left[\frac{(q_{e(exp)}-q_{e(cal)})}{q_{e(exp)}}\right]_i \tag{7}$$

(vii) The sum of absolute error (EABS)

$$\sum_{i=1}^{N}[q_{e(exp)}-q_{e(cal)}]_i \tag{8}$$

(viii) The average percentage error (APE)

$$\sum_{i=1}^{N}\frac{[(q_{e(exp)}-q_{e(cal)})/q_{e(exp)}]_i}{N}\times 100 \tag{9}$$

The calculation method for the 'sum of the normalized errors' was as follows:

(a) Select one isotherm and one error function and determine the isotherm parameters that minimize the error function for that isotherm to produce the isotherm parameter set for that error function.
(b) Determine the values for all the other error functions for that isotherm parameter set.
(c) Calculate all other parameter sets and all their associated error function values for that isotherm.
(d) Select each error measure in turn and ratio the value of that error measure for a given parameter set to the largest value of that error from all the parameter sets for that isotherm.
(e) Sum all these normalized errors for each parameter set.

The parameter set thus providing the smallest normalized error sum can be considered to be optimal for that isotherm provided.

3. Result and discussion

3.1. Characterization of CVM and MVM

A SEM study shows (Figs. 2a and 2b) that both CVM and MVM have considerable number of heterogeneous pores where there is a good possibility for dye to be trapped and adsorbed (Hameed and El-Khaiary, 2008). This figure reveals that the MVM shows much more rough irregular in shape and porous as compared to CVM.

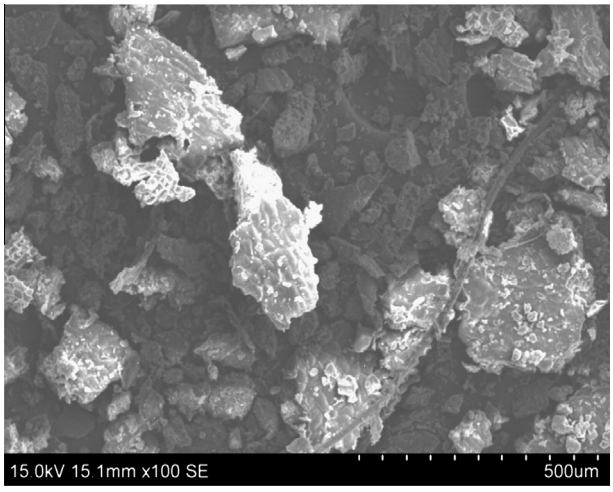

Figure 2a SEM image of CVM.

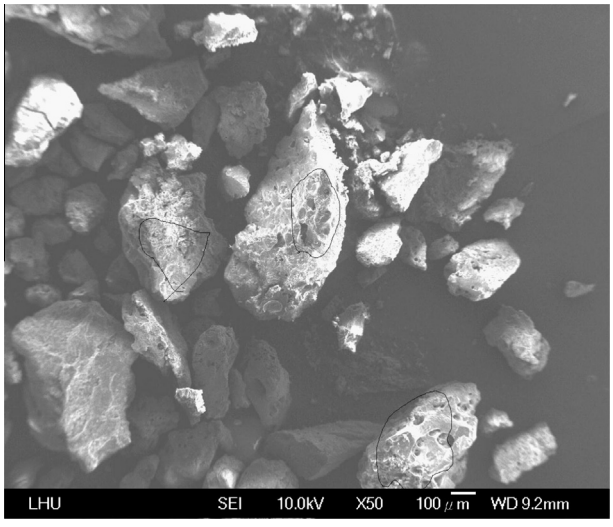

Figure 2b SEM image of MVM.

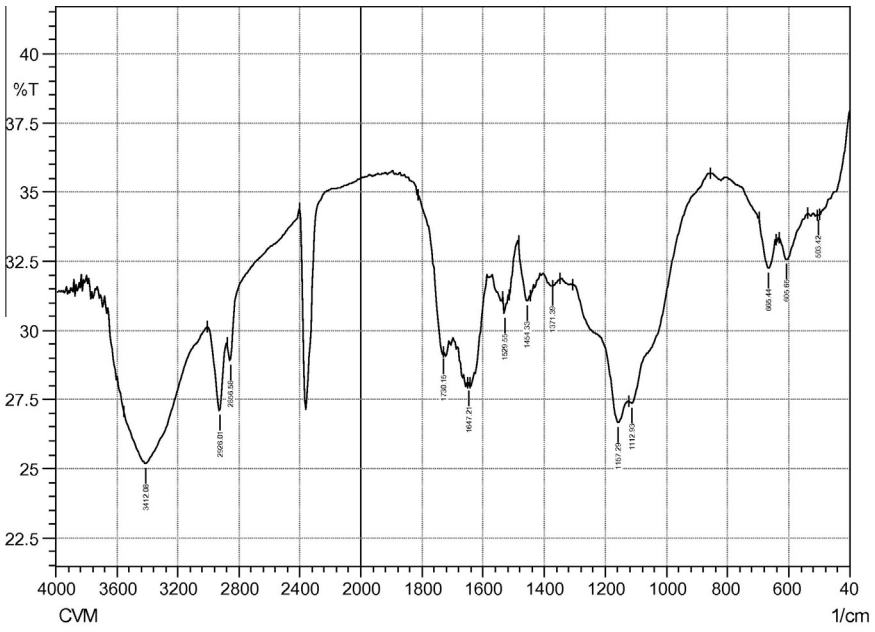

Figure 3a FTIR spectra of CVM.

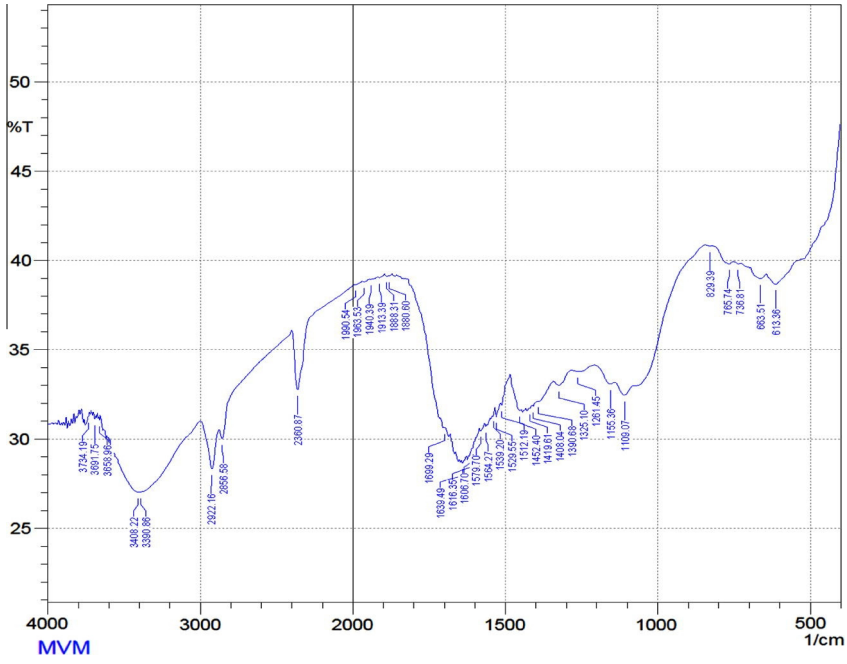

Figure 3b FTIR spectra of MVM.

The FTIR spectra of CVM and MVM are presented in Figs. 3a and 3b. The band at 3412 cm^{-1} represents the presence of –OH and –NH groups. The band observed at 2926 and 2856 cm^{-1} is associated to asymmetric and symmetric stretching vibrations of –CH group of both carbons (Ahmad and Kumar, 2010). Atmospheric CO_2 bands are present at 2360 cm^{-1} (antisymmetric C═O stretch) was observed for MVM only. The bands at 1637 and 1452 cm^{-1} indicate the presence of –COO, –C═O and –NH groups for CVM and MVM. The peak at 1564 cm^{-1} is attributed to the formation of oxygen functional groups such as a highly conjugated C–O stretching in carboxylic groups (Freundlich, 1960) and due to the presence of quinone structure. The bands at 1390–1408 cm^{-1} are assigned to C–H bending in alkanes or alkyl groups were observed in MVM. The broad band between 1325 and 1109 cm^{-1} has been assigned to C–O stretching in alcohols and phenols (Freundlich, 1960; Shelden et al., 1993). Another absorption band appearing around 1261 and 663 cm^{-1} can be attributed to the Si–C stretch and C–O–H twist. The band at 1261 cm^{-1} implied the C–N stretching of

Table 1 Physico-chemical characteristics of CVM and MVM.

Parameters	CVM	MVM
Moisture content (%)	21.713	8.713
Ash content (%)	5.950	9.950
pH	6.800	7.020
Decolorizing power (mg g^{-1})	1.100	1.200
Specific gravity	1.240	1.220
Water soluble matter (%)	13.44	12.44
Conductivity (μS cm^{-1})	0.210	0.260
Zero point charge (pH_{zpc})	3.800	4.400
Apparent density (g mL^{-1})	0.256	0.272

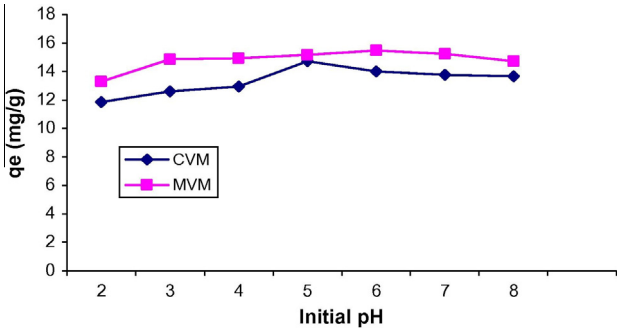

Figure 4a Effect of pH on the adsorption of CV onto CVM and MVM.

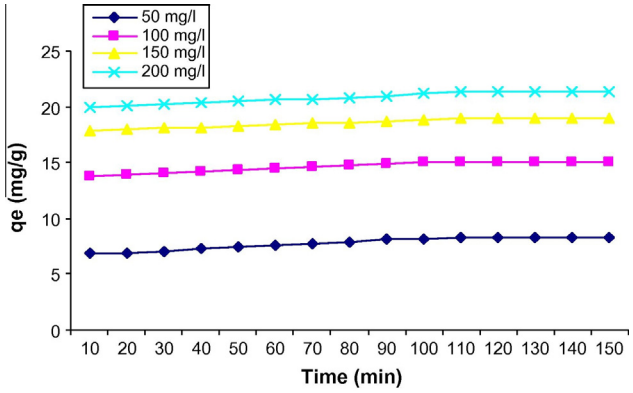

Figure 4b Effect of contact time and initial concentration on the adsorption of CV onto CVM.

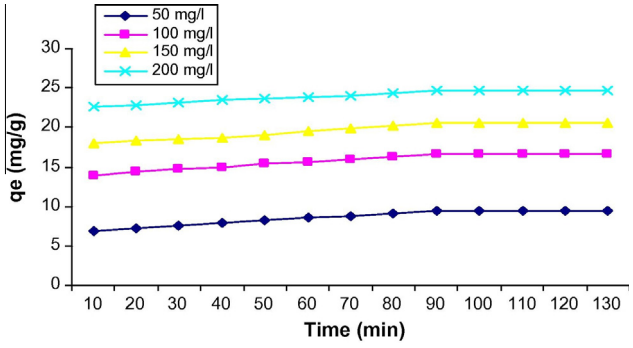

Figure 4c Effect of contact time and initial concentration on the adsorption of CV onto MVM.

amide similarly present in MVM. The characteristics of CVM and MVM are presented in Table 1.

3.2. Effect of pH on the adsorption of CV onto CVM and MVM

The adsorption capacity increased with increase in solution pH and the maximum adsorption capacity for CV was observed at 5 pH onto CVM and 6 pH onto MVM depicted in Fig. 4a. The effect of solution pH is very important when the adsorbing molecules are capable of ionizing in response to the current pH. When solution pH increases, high OH^- ions accumulate on the adsorbent surface (Ahmad and Kumar, 2010). Therefore, electrostatic interaction between negatively charge adsorbent surface and cationic dye molecules increases the adsorption (Santhi et al., 2010). Furthermore, the solution pH is above the zero point charge (pH_{zpc} = 3.8 for CVM and 4.4 for MVM) and hence the negative charge density of the surface of the adsorbents increased which favors the adsorption of cationic dye (Janos et al., 2003). The optimum pH value of CV onto CVM and MVM was 5 and 6 pH, respectively.

3.3. Effect of contact time and initial dye concentration

The uptake of CV onto CVM and MVM as a function of contact time is shown in Figs. 4b and 4c. It can be seen that the amount of CV adsorbed per unit mass of adsorbent increased with increasing dye concentration, although percentage removal decreased with increase in initial dye concentration. The uptake of CV was increased from 6.83 to 19.97 mg g^{-1} for CVM and 6.89 to 22.56 mg g^{-1} for MVM with the increase in CV concentration from 50 to 200 mg L^{-1}. This may be attributed to an increase in the driving force of the concentration gradient with the increase in the initial dye concentration (Hameed et al., 2008).

The uptake of CV onto CVM and MVM was increased with the increase in contact time. The adsorption equilibrium was achieved 110 min for CVM and 90 min for MVM. So compared to MVM, CVM is more time consuming and also the percentage of dye removal is less. Initial adsorption was rapid due to the adsorption of dye onto exterior surface, after that dye molecules enter into pores (interior surface), relatively slow process (Ahmad and Kumar, 2010). Data on the adsorption kinetics of dyes by various adsorbents have shown a wide

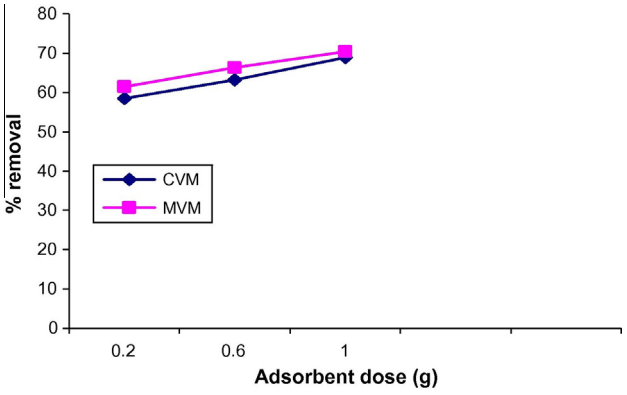

Figure 4d Effect of adsorbent dose on the adsorption of CV onto CVM and MVM.

Table 2 Isotherm constants for adsorption of CV onto 0.2 g of CVM and MVM.

Isotherm model	CVM	MVM
Langmuir		
Q_m (mg g^{-1})	30.4878	38.0228
b (L mg^{-1})	0.0193	0.0158
R^2	0.9793	0.9998
Freundlich		
$1/n$	0.6313	0.9371
K_F (mg g^{-1})	1.1920	1.0819
R^2	0.9456	0.9717
Dubinin–Radushkevich		
Q_m (mg g^{-1})	16.8928	18.0307
K ($\times 10^{-5}$ mol^2 kJ^{-2})	2.0000	2.0000
E (kJ mol^{-1})	0.15811	0.15811
R^2	0.8770	0.8318

range of adsorption rates. For example, the effect of contact time for the adsorption of orange-G and crystal violet dye by bagasse fly ash was studied for a period of 24 h for initial dye concentrations of 10 mg L^{-1} at 30 °C (Mall et al., 2006). The authors Mall et al. (2006) reported that after 4 h of contact, a steady-state approximation was assumed and a quasi-equilibrium situation was accepted.

3.4. Effect of adsorbent dose on dyes adsorption

The adsorption of CV onto CVM and MVM was studied by changing the quantity of adsorbent (0.2, 0.6 and 1 g) in the test solutions while keeping the initial dyes concentration 100 mg L^{-1} (Fig. 4d). It was observed that the percentage removal increases with increase in adsorbent dose. The increase in % color removal was due to the increase of the available sorption surface and availability of adsorption sites (Hameed, 2009). A similar observation was previously reported from the removal of malachite green dye from aqueous solution by bagasse fly ash and activated carbon (Mall et al., 2005).

3.5. Adsorption isotherm

To optimize the design of an adsorption system for the adsorption of adsorbates, it is important to establish the most appropriate correlation for the equilibrium curves (Altinisik et al., 2010). The equation parameters of these equilibrium models often provide some insight into the sorption mechanism, the surface properties and the affinity of the adsorbent (Bulut et al., 2008). Langmuir, Freundlich, and Dubinin–Radushkevich (D–R) were used to describe the equilibrium characteristics of adsorption.

3.5.1. The Langmuir isotherm

The Langmuir isotherm theory assumes monolayer coverage of adsorbate over a homogeneous adsorbent surface (Langmuir, 1918). A basic assumption is that sorption takes place at specific homogeneous sites within the adsorbent. Once a dye molecule occupies a site, no further adsorption can take place at that site. The Langmuir adsorption isotherm has been successfully used to explain the adsorption of basic dyes from aqueous solutions (Tan et al., 2007; Hameed et al., 2007). It is commonly expressed as followed:

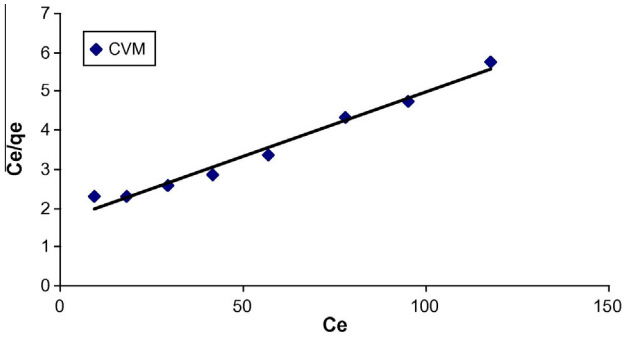

Figure 5a Langmuir adsorption isotherm for CV onto CVM.

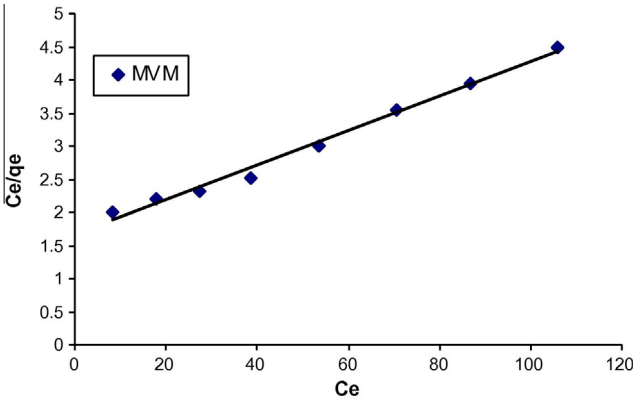

Figure 5b Langmuir adsorption isotherm for CV onto MVM.

$$q_e = (Q_m K_a C_e)/(1 + K_a C_e) \quad (10)$$

The Langmuir isotherm equation (10) can be linearized into the following form (Kinniburgh, 1986):

$$C_e/q_e = 1/K_a Q_m + (1/Q_m \times C_e) \quad (11)$$

where q_e and C_e are defined before in Eq. (1), Q_m is a constant and reflects a complete monolayer (mg g^{-1}); K_a is adsorption equilibrium constant (L mg^{-1}) that is related to the apparent energy of sorption. A plot of C_e/q_e versus C_e should indicate a straight line of slope $1/Q_m$ and an intercept of $1/(K_a Q_m)$.

The results obtained from the Langmuir are shown in Table 2 and the theoretical Langmuir isotherm is plotted in Figs. 5a and 5b together with the experimental data points. The related error function values (Table 3) are near the experimental adsorbed amounts and correspond closely to the adsorption isotherm plateau, which is acceptable. The correlation coefficient showed strong positive evidence on the adsorption of CV onto CVM and MVM follows the Langmuir isotherm. The applicability of the linear form of Langmuir model to CVM and MVM was proved by the high correlation coefficient $R^2 = 0.9793$ and 0.9998 for CV adsorption. This suggests that the Langmuir isotherm provides a good model of the sorption system. The maximum monolayer capacity Q_m obtained from Langmuir is 30.4878 mg g^{-1} for CV onto CVM and 38.0228 mg g^{-1} for CV onto MVM, respectively.

3.5.2. The Freundlich isotherm

The Freundlich isotherm (Freundlich, 1960) can be applied to non-ideal adsorption on heterogeneous surfaces as well as

Table 3 Values of error function of the isotherm models of CV onto CVM and MVM.

Adsorbent	Error function model	Isotherm model		
		Langmuir	Freundlich	D–R
CVM	RMSE	6.7015	22.2836	27.64
	χ^2	0.16421	25.2747	52.3829
	ERRSQ	2.594	102.612	134.8966
	HYBRD	0.18285	7.23150	9.5066
	MPSD	0.0128	0.5096	0.66996
	ARE	0.1135	0.71388	0.8185
	EABS	1.6108	10.1298	11.6145
	APE	1.4189	8.9235	10.231
MVM	RMSE	7.3788	20.9144	31.5652
	χ^2	0.1697	13.6556	46.78094
	ERRSQ	2.8905	84.1035	148.0079
	HYBRD	0.18855	5.48631	9.6549
	MPSD	0.01230	0.3588	0.62955
	ARE	0.11090	0.59823	0.79344
	EABS	1.70016	9.1708	12.16585
	APE	1.3863	7.47796	9.92016

multilayer sorption. The Freundlich isotherm can be derived assuming a logarithmic decrease in enthalpy of adsorption with the increase in the fraction of occupied sites and is commonly given by the following non-linear equation:

$$q_e = K_F C_e^{1/n} \tag{12}$$

Eq. (12) can be linearized in the logarithmic form (Eq. (13)) and the Freundlich constants can be determined:

$$\log q_e = \log K_F + \frac{1}{n} \log C_e \tag{13}$$

A plot of $\log q_e$ versus $\log C_e$ (Figs. 5c and 5d) enables to determine the constant K_F and $1/n$. K_F is roughly an indicator of the adsorption capacity, related to the bond energy and $1/n$ is the adsorption intensity of dye onto the adsorbent or surface heterogeneity. The magnitude of the exponent, $1/n$, gives an indication of the favorability of adsorption. Value of $1/n < 1$ represent favorable adsorption condition (Ho and McKay, 1978). The data obtained from linear Freundlich isotherm for the adsorption of the CV onto CVM and MVM is presented in Table 2. The comparability of the Freundlich model to the Langmuir model was proved by the correlation coefficient $R^2 = 0.9456$ and 0.9717 for adsorption of CV onto CVM and MVM. The $1/n$ value is lower than unity, indicating the favorable adsorption process as it is equal to 0.6313 for CV onto CVM and 0.9371 for CV onto MVM. It is lower than the experimental amounts corresponding to the adsorption isotherm plateau, which is unacceptable.

3.5.3. The Dubinin–Radushkevich (D–R) isotherm

The D–R isotherm was also applied to estimate the porosity apparent free energy and the characteristics of adsorption (Dubinin, 1960, 1965; Radushkevich, 1949). It can be used to describe adsorption on both homogenous and heterogeneous surfaces (Shahwan and Erten, 2004). The D–R equation can be defined by the following equation:

$$\ln q_e = \ln Q_m - K\varepsilon^2 \tag{14}$$

where K is a constant related to the adsorption energy, Q_m the theoretical saturation capacity, ε the Polanyi potential, calculated from Eq. (15):

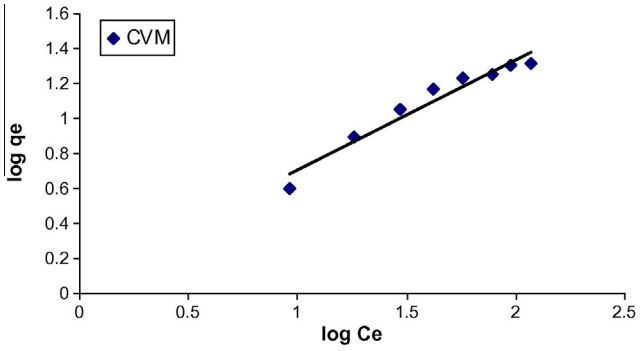

Figure 5c Freundlich adsorption isotherm for CV onto CVM.

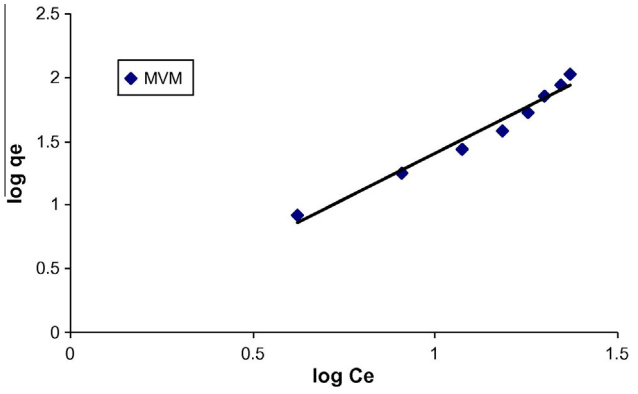

Figure 5d Freundlich adsorption isotherm for CV onto MVM.

$$\varepsilon = RT \ln\left(1 + \frac{1}{C_e}\right) \tag{15}$$

where C_e is the equilibrium concentration of dye (mol L^{-1}), R *is the* gas constant (8.314 J mol^{-1} K^{-1}) and T is the temperature (K). By plotting $\ln q_e$ versus ε^2, it is possible to determine the value of K from the slope and the value of Q_m (mg g^{-1})

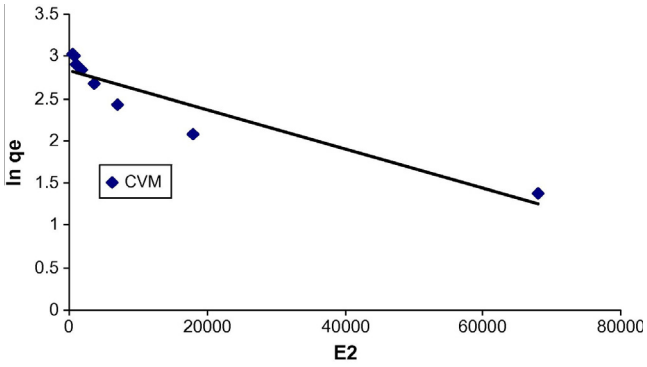

Figure 5e D–R adsorption isotherm for CV onto CVM.

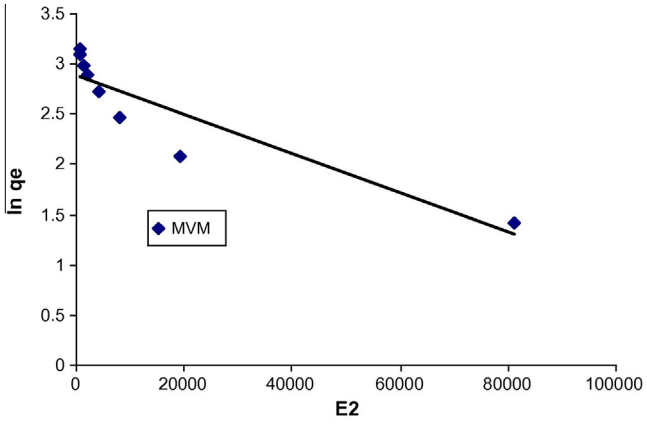

Figure 5f D–R adsorption isotherm for CV onto MVM.

from the intercept (Figs. 5e and 5f). The mean free energy E (kJ mol^{-1}) of sorption can be estimated by using K values as expressed in the following equation (Hobson, 1969):

$$E = \frac{1}{\sqrt{2K}} \tag{16}$$

The parameters obtained using above equations was summarized in Table 2. The saturation adsorption capacity Q_m obtained using D–R isotherm model for CV onto CVM is 16.8928 mg g^{-1} and MVM is 18.0307 mg g^{-1}. The E values calculated using Eq. (16) are 0.15811 kJ mol^{-1} for both CV adsorption onto CVM and MVM. This was indicating that the physical adsorption plays the significant role in the uptake of CV onto CVM and MVM. The error functions indicate that the D–R isotherm is not fit in this adsorption.It can be seen that the Langmuir isotherm fits the data better than Freundlich and D–R isotherms. The fact that it may be due to the predominantly homogeneous distribution of active sites on the activated carbons surfaces; since the Langmuir equation assumes that the adsorbent surface is energetically homogeneous. This is also confirmed by the high value of R^2 (Table 2). This indicates that the adsorption of CV onto CVM and MVM takes place as monolayer adsorption.

Over the past few decades, linear regression has been developed as a major option in designing the adsorption systems. However, recent investigations have indicated the growing discrepancy (between the predictions and experimental data) and disability of the model, propagating toward a different outcome. However the expanding of the non-linear isotherms represents a potentially viable and powerful tool, leading to the superior improvement in the area of adsorption science (Foo and Hameed, 2010).

Table 4 Reported maximum adsorption capacities (Q_m in mg g^{-1}) in the literature for cationic dye obtained on low-cost adsorbents.

Adsorbent	Q_m (mg g^{-1})	References
MVM	38.0228	This study
CVM	30.4878	This study
Luffa cylindrical	9.920	Altinisik et al. (2010)
Coffee ground activated carbon	23.00	Reffas et al. (2010)
Kolin	5.44	Gupta et al. (2008)
Wheat bran	22.73	Gupta et al. (2007)
Rice bran	14.63	Gupta et al. (2007)
Hen feathers	26.10	Mittal (2006)
Arundo donax root carbon	8.69	Zhang et al. (2008)
Bentonite	7.72	Tahir and Rauf (2006)

The maximum sorption capacity (Q_m) of the adsorption of CV onto CVM and MVM was compared with those reported in literature (Table 4).

3.6. Adsorption kinetics

The kinetics of adsorbate uptake is important for choosing optimum operating conditions for design purposes. In order to investigate the mechanism of adsorption and potential rate controlling steps such as chemical reaction, diffusion control and mass transport process, kinetic models have been used to test experimental data from the adsorption of CV onto CVM and MVM. These kinetic models were analyzed using pseudo-first-order, pseudo-second-order and intraparticle diffusion.

3.6.1. Pseudo-first-order equation

The pseudo-first-order equation of Lagergren is generally expressed as follows:

$$\frac{dq_t}{d_t} = K_1(q_e - q_t) \tag{17}$$

where q_e and q_t (mg g^{-1}) are the adsorption capacity at equilibrium and at time t, respectively, k_1 (L min^{-1}) is the rate constant of pseudo-first-order adsorption. Integrating Eq. (17) for the boundary conditions $t = 0$–t and $q_t = 0$–q_t gives

$$\log\left(\frac{q_e}{q_e - q_t}\right) = \frac{K_1}{2.303}t \tag{18}$$

Eq. (18) can be rearranged to obtain the following linear form:

$$\log(q_e - q_t) = \log(q_e) - \frac{K_1}{2.303}t \tag{19}$$

The values of q_e and K_1 for the pseudo-first-order kinetic model were determined from the intercepts and the slopes of the plots of $\log(q_e - q_t)$ versus time (Figs. 6a and 6b). The K_1 values, R^2 values and q_e values (experimental and calculated) are summarized in Table 5.

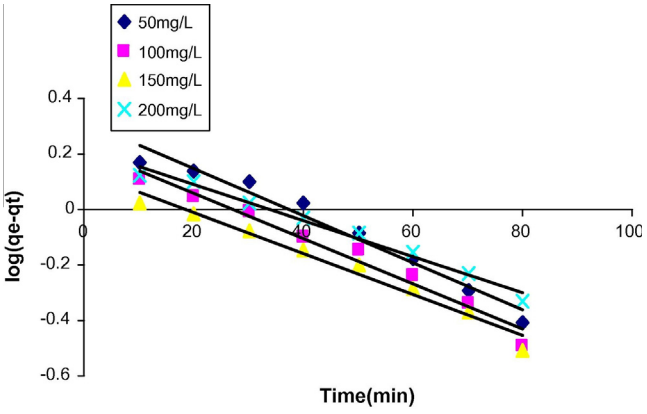

Figure 6a Pseudo-first-order kinetics at different initial concentrations for CV onto CVM.

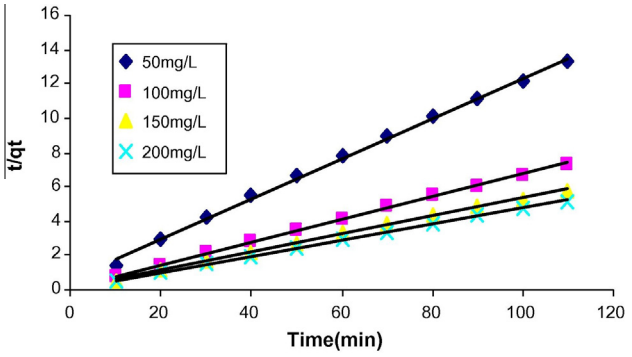

Figure 6c Pseudo-second-order kinetics at different initial concentrations for CV onto CVM.

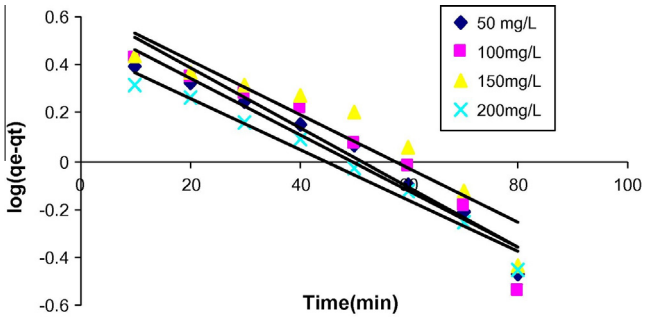

Figure 6b Pseudo-first-order kinetics at different initial concentrations for CV onto MVM.

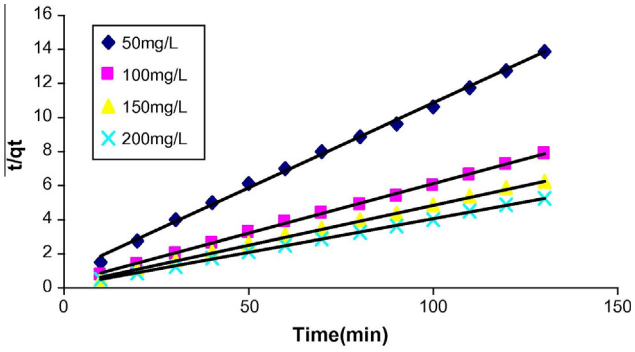

Figure 6d Pseudo-second-order kinetics at different initial concentrations for CV onto MVM.

3.6.2. Pseudo-second-order equation

The pseudo-second-order equation is generally given as follows:

$$\frac{dq_t}{d_t} = K_2(q_e - q_t)^2 \tag{20}$$

where K_2 (g mg^{-1} min^{-1}) is the second-order rate constant. Integrating Eq. (20) for the boundary conditions $q_t = 0$–q_t at $t = 0$–t is simplified as can be rearranged and linearized to obtain:

$$\frac{t}{q_t} = \frac{1}{K_2 q_e^2} + \frac{1}{q_e}(t) \tag{21}$$

The second-order rate constants were used to calculate the initial sorption rate, given by the following equation:

$$h = K_2 q_e^2 \tag{22}$$

The plot of t/q_t versus time is a straight line as shown in Figs. 6c and 6d. The K_2 and q_e values determined from the slopes and intercepts of the plot are presented in Table 5 along with the corresponding correlation coefficient. This procedure is more likely to predict the behavior over the whole range of adsorption. The linear plot shows a good agreement between the experimental and calculated q_e values (Table 5). The corresponding correlation coefficient (R^2) values for the pseudo-second-order kinetic model were greater than pseudo-first-order kinetic model for

Table 5 First- and second-order kinetic parameters for the adsorption of CV onto CVM and MVM at different initial concentrations.

Sorbent	C_0 (mg L^{-1})	$q_{e(exp)}$ (mg g^{-1})	Pseudo-first-order			Pseudo-second-order		
			K_1 (min)	$q_{e(cal)}$ (mg g^{-1})	R^2	K_2 (g mg^{-1} min^{-1})	$q_{e(cal)}$ (mg g^{-1})	R^2
CVM	50	7.5827	0.0196	2.0739	0.9636	0.0201	8.5763	0.9975
	100	14.4218	0.0189	1.6722	0.9706	0.02756	15.2207	0.9995
	150	18.3791	0.0168	1.3601	0.9710	0.0369	19.0476	0.9997
	200	20.6091	0.0147	1.6489	0.9851	0.0266	21.4132	0.9996
MVM	50	8.250	0.0269	3.7783	0.9577	0.0118	10.010	0.9977
	100	15.331	0.0285	4.3251	0.9123	0.0125	17.2117	0.9992
	150	19.413	0.0257	4.3471	0.8804	0.0113	21.3219	0.9991
	200	23.997	0.0244	2.9798	0.9729	0.0175	25.0629	0.9998

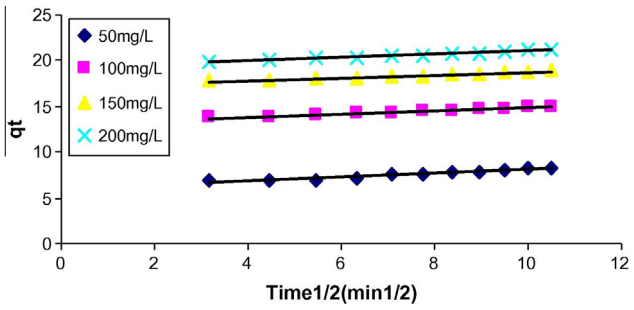

Figure 7a Intraparticle diffusion plot at different initial dye concentration for CV onto CVM.

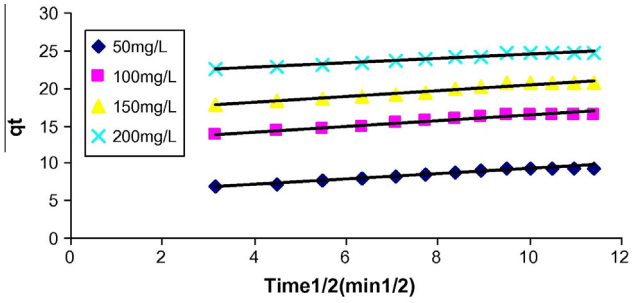

Figure 7b Intraparticle diffusion plot at different initial dye concentration for CV onto MVM.

all CV concentration, indicating the applicability of the pseudo-second-order kinetic model to describe the adsorption (Santhi et al., 2010). It suggested that the adsorption process was controlled by chemisorptions (Hameed, 2009).

3.6.3. Intraparticle diffusion

When the diffusion (internal surface and pore diffusion) of dye molecule inside the adsorbent is the rate-limiting step, then adsorption data can be presented by the following equation:

$$q_t = K_{dif} t^{1/2} + C \quad (23)$$

where C (mg g^{-1}) is the intercept and K_{dif} is the intraparticle diffusion rate constant (in mg g^{-1} min$^{-1/2}$). The values of q_t were found to be linearly correlated with values of $t^{1/2}$ (Figs. 7a and 7b) and the rate constant K_{dif} directly evaluated from the slope of the regression line (Table 6). The values of intercept C (Table 6) provide information about the thickness of the boundary layer and the resistance to the external mass

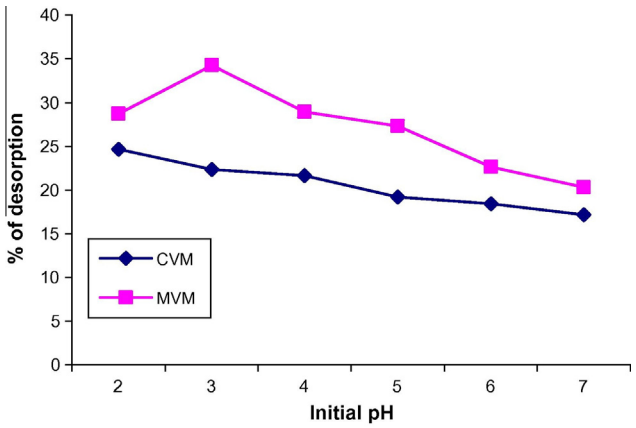

Figure 8 Desorption of CV onto CVM and MVM.

transfer increase as the intercept increase (Santhi et al., 2010). The constant C was found to increase from 5.9603 to 19.246 and 5.8535 to 21.66 with increase in CV concentration from 50 to 200 mg L^{-1} onto CVM and MVM, which indicating the increase of the thickness of the boundary layer and decrease of the chance of the external mass transfer and hence increase of the chance of internal mass transfer. The R^2 values are given in Table 6 are close to unity indicating the application of this model. This may confirm that the rate-limiting step is the intraparticle diffusion process. The linearity of the plots demonstrated that intraparticle diffusion played a significant role in the uptake of the CV onto CVM and MVM. However, as still there is no sufficient indication about it, Ho (2003) has shown that if the intraparticle diffusion is the sole rate-limiting step, it is essential for the q_t versus $t^{1/2}$ plots to pass through the origin, which is not the case in Figs. 7a and 7b, it may be concluded that surface adsorption and intraparticle diffusion were concurrently operating during the adsorbate and adsorbent interactions.

3.7. Desorption studies

Regeneration of the adsorbent may make the treatment more economical and feasible. Desorption studies help to elucidate the mechanism of dye adsorption and recycling of the spent adsorbent and the adsorbate. If the adsorbed dyes can be desorbed using neutral pH water, then the attachment of the dye to the adsorbent is by weak bonds. The maximum desorption of CV onto CVM (24.63%) and CV onto MVM (34.27%) is obtained at 2 and 3 pH, respectively (Fig. 8).

Table 6 Parameters of the intraparticle diffusion model for the adsorption of CV onto CVM and MVM.

Adsorbents	C_0 (mg L^{-1})	K_{dif}	C	R^2
CVM	50	0.2189	5.9603	0.9753
	100	0.1830	13.065	0.9854
	150	0.1494	17.272	0.9759
	200	0.1840	19.246	0.9646
MVM	50	0.3373	5.8536	0.9654
	100	0.3651	12.774	0.9618
	150	0.3859	16.559	0.9545
	200	0.2835	21.660	0.9681

3.8. Adsorption mechanism

The FTIR studies of the CVM and MVM have confirmed the presence of hydroxyl groups and carboxylic groups. The biosorption of CV onto CVM and MVM may be likely due to electrostatic attraction between these groups and the cationic dye molecules (CV^+). At pH above 4.4, the carboxyl groups are deprotonated and as such are negatively charged. These negatively charged carboxylate ligands ($-COO^-$) can attract the positively charged CV molecules and binding can occur. Thus the CV^+ binding to the CVM and MVM may be ion-exchange mechanism, which may involve electrostatic interaction between the negatively charged groups in the cell walls and the dye cationic molecules. There is the weak electrostatic interaction between the CV and the electron-rich sites of the adsorbent surface.

Activated carbons are materials which have amphoteric characteristics, so the pH on its surface always changes depending on initial pH of the solution. Generally, the adsorption capacity and rate constant have the tendency to increase as initial pH of the solution increases. This is due to the pH_{zpc} of the adsorbents which has an acidic value; this is favorable for cation adsorption (Prahas et al., 2008). It is commonly known fact that the anions are favorably adsorbed by the adsorbent at lower pH values due to presence of H^+ ions. At high pH values, cations are adsorbed due to the negatively charged surface sites of the adsorbents:

$$COO^- + CV^+ = COO\text{–}CV$$

4. Conclusion

The removal of CV from aqueous solution by using chemically and microwave activated *A. nilotica* leaves has been investigated for various parameters such as initial pH, contact time, adsorbent dosage and initial dye concentration. From this study, it was found that MVM has a higher adsorption efficiency compared to CVM at the any given parameters. The equilibrium data were best described by the Langmuir isotherm model, exclusively for all the error function selection methods. The adsorption kinetics can be successfully fitted to pseudo-second-order kinetic model. The result of the intraparticle diffusion model suggested that intraparticle diffusion was not the only rate controlling step. The recycling ability of MVM is greater than CVM. It reveals that recovery of the dye from adsorbent was possible. The *A. nilotica* leaves used in this work are freely and abundantly available. The preparation of MVM does not require an additional chemical treatment step and is agreeing with the principles of green chemistry. Therefore, the eco friendly adsorbent MVM is expected to be the environmentally and economically suitable for the removal of CV from aqueous solution.

References

Ahmad, R., Kumar, R., 2010. Adsorption studies of hazardous malachite green onto treated ginger waste. J. Environ. Manage. 91, 1032–1038.

Altinisik, A., Gur, Emel, Seki, Yoldas, 2010. A natural sorbent, *Luffa cylindrical* for the removal of a model basic dye. J. Hazard. Mater., doi:10.1016.

Bulut, E., Ozacar, M., Sengil, A.I., 2008. Adsorption of malachite green onto bentonite: equilibrium and kinetic studies and process design. Micropor. Mesopor. Mater. 115, 234–246.

Dubinin, M.M., 1960. The potential theory of adsorption of gases and vapors for adsorbents with energetically non-uniform surface. Chem. Rev. 60, 235–266.

Dubinin, M.M., 1965. Modern state of the theory of volume filling of micropore adsorbents during adsorption of gases and steams on carbon adsorbents. Zh. Fiz. Khim. 39, 1305–1317.

Foo, K.Y., Hameed, B.H., 2010. Insight into the modeling of adsorption isotherm systems. Chem. Eng. J. 156, 2–10.

Freundlich, H., 1960. Uber die adsorption in losungen (Adsorption in solution). Z. Phys. Chem. 57, 384–470.

Gupta, V.K., Ali, I., Saini, V.K., 2007. Adsorption studies on the removal of vertigo blue 49 and orange DNA 13 from aqueous solutions using carbon slurry developed from a waste material. J. Colloid Interf. Sci. 315, 87–93.

Gupta, V.K., Mittal, A., Krishnan, L., Mittal, J., 2008. Adsorption of basic Fuchsine using waste materials – bottom ash and de-oiled soya as adsorbents. J. Colloid Interf. Sci. 319, 30–39.

Hadi, Mahdi, Mohammad, R., Samarghandi, T., McKay, Gordon, in press. Equilibrium two-parameter isotherms of acid dyes sorption by activated carbons: study of residual errors. Chem. Eng. J. doi:10.1016/j.cej.2010.03.016.

Hameed, B.H., 2009. Spent tea leaves: a non-conventional and low-cost adsorbent for removal of basic dye from aqueous solutions. J. Hazard. Mater. 161, 753–759.

Hameed, B.H., El-Khaiary, M.I., 2008. Removal of basic dye from aqueous medium using a novel agricultural waste material: pumpkin seed hull. J. Hazard. Mater. 155, 601–609.

Hameed, B.H., Din, A.T.M., Ahmad, A.L., 2007. Adsorption of methylene blue onto bamboo-based activated carbon: kinetics and equilibrium studies. J. Hazard. Mater. 141, 819–825.

Hameed, B.H., Mahmoud, D.K., Ahmad, A.L., 2008. Sorption of basic dye from aqueous solution by pomelo (*Citrus grandis*) peel in a batch system, colloids. Colloids Surf. A: Physicochem. Eng. Aspects 316, 78–84.

Ho, Y.S., 2003. Removal of copper ions from aqueous solution by tree fern. Water Res. 37, 2323–2330.

Ho, Y.S., 2004. Selection of optimum sorption isotherm. Carbon 42, 2115–2116.

Ho, Y.S., McKay, G., 1978. Sorption of dye from aqueous solution by peat. Chem. Eng. J. 70, 115–124.

Hobson, J.P., 1969. Physical adsorption isotherms extending from ultrahigh vacuum to vapor pressure. J. Phys. Chem. 73, 2720–2727.

Janos, P., Buchtova, H., Ryznarova, M., 2003. Sorption of dye from aqueous solution onto fly ash. Water Res. 37, 4938–4944.

Khan, A.R., Al-Waheab, I.R., Al-Haddad, A., 1996. A generalized equation for adsorption isotherms for multi-component organic pollutants in dilute aqueous solution. Environ. Technol. 17, 13–23.

Kinniburgh, D.G., 1986. General purpose adsorption isotherms. Environ. Sci. Technol. 20, 895–904.

Langmuir, I., 1918. The adsorption of gases on plane surface of glass, mica and platinum. J. Am. Chem. Soc. 40, 1361–1403.

Madhavakrishnan, S., Manickavasangam, K., Vasanthakumar, R., et al., 2009. Adsorption of crystal violet dye from aqueous solution using *Ricinus communis* pericarp carbon as an adsorbent. Eur. J. Chem. 6 (4), 1109–1116.

Malek, A., Farooq, S., 1996. Comparison of isotherm models for hydrocarbon adsorption on activated carbon. AlChE J. 42, 431–441.

Mall, I.D., Srivastava, V.C., Agarwal, N.K., Mishra, I.M., 2005. Adsorptive removal of malachite green dye from aqueous solution by bagasse fly ash and activated carbon – kinetic study and equilibrium isotherm analyses. Colloids Surf. A: Physicochem. Eng. Aspects 264, 17–28.

Mall, I.D., Srivastava, V.C., Agarwal, N.K., 2006. Removal of orange-G and crystal violet dye by adsorption onto bagasse fly ash – kinetic study and equilibrium isotherm analyses. Dyes Pigments 69, 210–223.

Mittal, A., 2006. Adsorption kinetics of removal of a toxic dye, malachite green, from waste water by using hen feathers. J. Hazard. Mater. B 133, 196–202.

Ncibi, M.C., 2008. Applicability of some statistical tools to predict optimum adsorption isotherm after linear and non-linear regression analysis. J. Hazard. Mater. 153, 207–212.

Prahas, D., Kartika, Y., Indraswati, N., Ismadji, S., 2008. The use of activated carbon prepared from jackfruit (*Artocarpus heterophyllus*) peel waste for methylene blue removal. J. Environ. Prot. Sci. 2, 1–10.

Puri, S., Bangarwa, K.S., Singh, S., 1995. Influence of multipurpose trees on agricultural crops in arid regions of Haryana, India. I. Arid Environ. 30, 441–451.

Radushkevich, L.V., 1949. Potential theory of sorption and structure of carbons. Zh. Fiz. Khim. 23, 1410–1420.

Reffas, A., Bernardet, V., David, B., et al., 2010. Carbon prepared from coffee grounds by H_3PO_4 activation: characterization and adsorption of methylene blue and nylosan red N-2RBL. J. Hazard. Mater. 175, 779–788.

Santhi, T., Manonmani, S., Smitha, T., 2010. Removal of malachite green from aqueous solution by activated carbon prepared from the epicarp of *Ricinus communis* by adsorption. J. Hazard. Mater. 179, 178–186.

Seidel, A., Gelbin, D., 1988. On applying the ideal adsorbed solution theory to multi-component adsorption equilibria of dissolved organic components on activated carbon. Chem. Eng. Sci. 43, 79–89.

Seidel-Morgenstern, A., Guichon, G., 1993. Modelling of the competitive isotherms and the chromatographic separation of two enantiomers. Chem. Eng. Sci. 48, 2787–2797.

Selen, M.A.G.U., de Souza Peruzzo, L.C., de Souza Antonio, A.U., 2008. Numerical study of the adsorption of dyes from textile effluents. Appl. Math. Modell. 32, 1711–1718.

Shahwan, T., Erten, H.N., 2004. Temperature effects on barium sorption on natural kalinite and chlorite-illite clays. J. Radioanal. Nucl. Chem. 260, 43–48.

Shelden, R.A., Caseri, W.R., Suter, U.W., 1993. Ion exchange on muscovite mica with ultrahigh specific surface area. J. Colloid Interf. Sci. 157 (2), 318–327.

Tahir, S.S., Rauf, N., 2006. Removal of cationic dye from aqueous solution by adsorption onto bentonite clay. Chemosphere 63, 1842–1848.

Tan, I.A.W., Hameed, B.H., Ahmad, A.L., 2007. Equilibrium and kinetic studies on basic dye adsorption by oil palm fibre activated carbon. Chem. Eng. J. 127, 111–119.

Tsai, S.C., Juang, K.W., 2000. Comparison of linear and non-linear forms of isotherm models for strontium sorption on a sodium bentonite. J. Radioanal. Nucl. Chem. 243, 741–746.

Zhang, J., Li, Y., Zhang, C., Jing, Y., 2008. Adsorption of malachite green from aqueous solution onto carbon prepared from Arundo donax root. J. Hazard. Mater. 150, 774–782.